fluenza will be most closely related to future strains is not necessarily equivalent to predicting the epidemic strain for the subsequent year. Strains may persist for several years, and a strain that is part of the epidemic one year may not represent the future course of the main trunk lineage of the virus. However, their method does predict with reasonable accuracy which current strain will eventually be most closely related to that causing future outbreaks of influenza. Thus, this method can be used in conjunction with standard epidemiological data to select strains of influenza for producing effective vaccines in advance of influenza epidemics. This would greatly help in the production of vaccines that are efficacious.

The ability to make predictions about the future evolutionary course of influenza is the latest example of the many practical applications of evolutionary biology. Evolution isn't just something that happened in the past; evolution can be observed in the present, and in some cases, used to predict the future. In the medical sciences, topics such as in vitro evolution of pharmaceuticals, drug resistance, emerging diseases, and epidemiological studies of pathogens all require a thorough understanding of evolutionary biology. More broadly within biology, an evolutionary perspective is needed to derive general principles from the huge amount of work that is conducted on model organisms, or to interpret any work that compares data across genes, individuals, populations, or species. School boards and science educators need to understand this simple fact: If students don't learn about evolution, they can't possibly understand modern biology or medicine.

References and Notes

1. R. M. Bush, C. A. Bender, K. Subbarao, N. J. Cox, W. M. Fitch, *Science* **286**, 1921 (1999).
2. W. M. Fitch *et al.*, *Proc. Natl. Acad. Sci. U.S.A.* **94**, 7712 (1997).
3. T. Zhu *et al.*, *Nature* **391**, 594 (1998).
4. N. K. Sauter *et al.*, *Biochemistry* **31**, 9609 (1992).
5. P. J. Kraulis, *J. Appl. Crystallogr.* **24**, 946 (1991).

PERSPECTIVES: PROTEIN STRUCTURE

Class-Conscious TCR?

Ian A. Wilson

The T cell receptor (TCR) recognizes peptides of processed antigen bound to class I or class II MHC (major histocompatibility complex) molecules on antigen presenting cells. Structural studies show that the TCR makes a diagonal footprint (buried imprint) on the surface of the peptide–MHC class I complex (*1*–*6*). This diagonal footprint (see figure, this page) enables the TCR both to interact with conserved MHC molecules and to discriminate between different antigenic peptides. The structure of the TCR bound to the peptide–MHC class I complex reveals that the genetically more diverse regions of the TCR (the central hypervariable loops, CDR 3α and 3β) interact most closely with peptide, whereas the less-variable CDR 1 and 2 regions interact with the α helices of MHC class I. The CDR 3α and 3β regions could interact with peptide in any number of orientations but to maintain the specificity of immune recognition, the number of orientations needs to be restricted. This could be accomplished by the interaction of the TCR–peptide MHC complex with coreceptors CD4 or CD8 on the T cell or through steric constraints imposed by extensive glycosylation of both the TCR and MHC (*7*). Now, Reinherz *et al.* report on page 1913 (*8*) the crystal structure at 3.2 Å of the variable region of the TCR D10 interacting with mouse MHC class II (I-A^k) bound to peptide antigen. The investigators propose that the orthogonal orientation of the TCR–class II interaction is more conserved than the diagonal orientation of the TCR–class I interaction. Differing specificities of TCR for MHC class II versus class I would then direct differentiation of T lymphocytes into either $CD4^+$ (helper) or $CD8^+$ (cytotoxic) cells, respectively.

Comparison of the new structure with the three previous TCR–peptide MHC class I structures—mouse 2C (*1*, *3*), human A6 (*2*) and B7 (*4*)—reveals both similarities and differences. Even within this rather small structural database, the range of TCR orientations extends from diagonal to almost orthogonal (see figure, next page). There are several ways in which the TCR variable region of the β chain (Vβ)—composed of CDR 1β, 2β, and 3β—has been seen to interact with the peptide-MHC complex. For example, Vβ of the mouse TCR 2C makes only a few interatomic contacts with either the peptide or MHC. In the human TCR A6 there is almost no contact between CDR 1β and 2β and the peptide-MHC, but, because of its larger size, CDR 3β dominates the Vβ interaction. Similarly, in the complex of TCR with B7, the Vβ region makes minimal contacts with the MHC, whereas CDR 3β makes extensive contacts with the peptide. For the interaction of TCR D10 with MHC class II, the size of the buried surface area by itself does not tell the whole story. CDR 2β and 3β dominate the interactions with the MHC helices, but have extraordinarily little contact with peptide. Thus, even though the surface area of Vβ buried in the MHC-peptide complex (338 A^2) is in the middle of those observed for the class I TCRs (260 to 430 A^2), the complementarity of the interface (0.70 versus 0.45 to 0.64) is much better than for other TCR–peptide MHC pairs (*8*).

So, how can the different interactions of TCRs with peptide-MHC complexes be consistent with a standard overall orientation? The variable loops of TCR's α chain (Vα) maintain a relatively constant and significant van der Waals interaction with both peptide and MHC in all four complexes. It appears that Vα dictates the overall orientation and that the position of Vβ is additionally modulated by the pair-

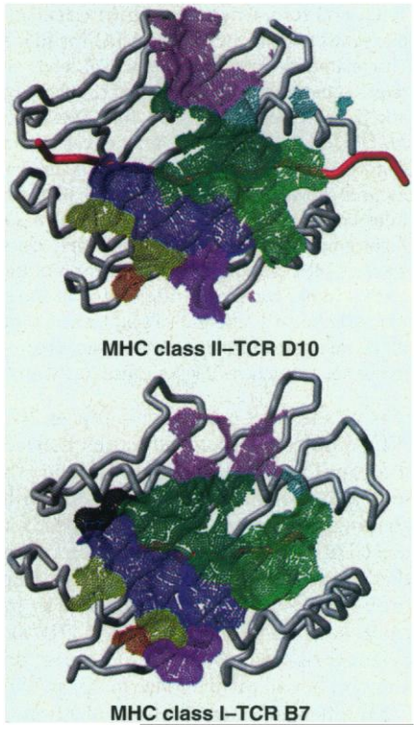

Footprints in the sand. Comparison of the footprint of a class II TCR D10 (*8*) and a class I TCR B7 (*4*) on their respective MHC molecules. The surface of the CDR variable loops are shown in dark blue (1α), dark purple (2α), dark green (3α), orange (4α), light blue (1β), light purple (2β), and light green (3β). The 27α and 51α residues are in yellowish-green, the amino-terminus of the α chain in B7 is in black, and the peptides in red. Figure calculated with MS (*11*) and rendered with MIDAS (*12*).

The author is at the Department of Molecular Biology and Skaggs Institute for Chemical Biology, The Scripps Research Institute, La Jolla, CA 92037, USA. E-mail: wilson@scripps.edu

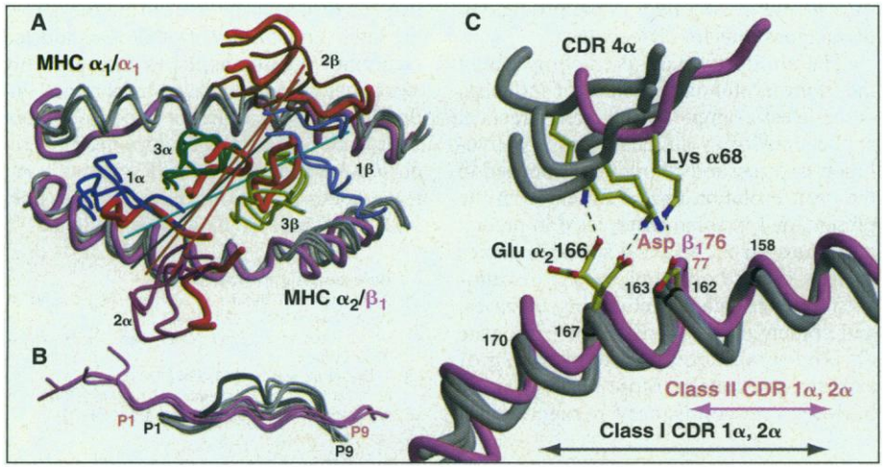

Twist and turn. Orientation of the class I and class II TCRs and the respective peptide-MHC complexes with which they interact. (**A**) The four structures were superimposed on their β-sheet floors. The relative orientations of the CDR loops are shown on top of the MHC peptide binding groove represented by the long opposing α helices (gray) of α_1 and α_2 for class I (H-2K^b, HLA-A2), and α_1 and β_1 (pink) for class II (I-E^k). The CDRs of TCR D10 are shown by a thick red tube and the 2C (*3*), A6 (*2*), and B7 (*4*) CDRs by thinner tubes, and are color coded as follows: 1α (dark blue), 2α (magenta), 3α (green), 1β (light blue), 2β (brown), and 3β (yellow). The principal axis of the TCR CDR loops is shown by a rod for D10 (red), B7 (orange), A6 (gray), and 2C (cyan). (**B**) Comparison of peptides bound to MHC class I and class II. A subset of conformations for peptide bound to murine (light gray), and human (dark gray) MHC class I and murine class II (pink) are shown with their respective MHC removed. (**C**) Comparison of the interaction of TCR CDR 4α with class I (gray) versus class II (pink) complexes. The switch in the salt bridge (from Lys α68) allows the Vα to ratchet around to form a different salt bridge but with the same helical segment in MHC class I versus class II. The numbered residues on the helices represent contacts with TCR loop residues 27α and 51α in the various structures. Figure calculated with MOLSCRIPT (*13*) and rendered with RASTER3D (*14*).

ings of the TCR's αβ chains (up to 20°). As a result, the footprint varies between diagonal and orthogonal. Indeed, the molecular orientation of the TCR can be strikingly different, but the positions of the CDR loops and the TCR footprint on the peptide-MHC complex are still approximately diagonal (bottom left to top right, both figures). So, the TCR D10 story suggests an orthogonal molecular orientation but an off-diagonal footprint (*8*).

The new structure focuses attention on the interaction of Vα with the MHC α_2 helix of class I and the corresponding β_1 helix of class II (see figure, this page). The Vα CDRs 1α, 2α, and 4α are directed toward a few turns of helix that are highly conserved within each MHC class, but are quite different between class I and class II. In most class I structures, the CDR 1α loop sits between the α_1 and α_2 helices (see figure, this page) and interacts significantly with peptide, whereas in the TCR D10 structure, the CDR 1α has shifted over because of the potential clash with the longer class II peptide, as it extends out above the floor of the groove. However, the main structural difference in the peptide binding groove between MHC class I and class II is around the amino terminus of the first long helix of class I α_1, which becomes a β strand and shorter α_1 helix in class II (see figure A, this page). This unique class II feature is surprisingly not recognized by TCR D10.

Given that the range of orientations appears to fall between orthogonal and diagonal, the main problem is how to predict such interactions. The peptide conformation itself is much more variable in class I than in class II; substantial variation occurs in the middle of the peptide for class I, but at the ends of the peptide for class II (see figure B, this page). The class I TCRs seem to have addressed that structural challenge by varying the length of their central CDR 3β and by reducing the extent to which CDR 1β and 2β interact with the MHC helices. The Reinherz proposal (*8*) of a more conserved orientation for the class II–TCR interaction is certainly consistent with the more uniform class II peptide conformation of the central P1 to P9 residues seen in all class II human and mouse MHCs. Thus, CDR contacts to both peptide and MHC helices can be maintained without the need to accommodate the variable bulges seen in class I peptides. However, a restricted TCR class II orientation also implies little variation in either the αβ chain pairing or the length of CDR 3β.

Reinherz *et al.* also propose that the TCR class-specific orientation can direct the maturation of either CD4$^+$ or CD8$^+$ T cells. Previously, it was noted that a switch between the CD4$^+$ and CD8$^+$ T cell classes [reviewed in (*9*)] resulted from substitution of TCR residues 27 and 51 at the tips of the CDR 1α and 2α loops (see figure, previous page). Although the TCR 27α and 51α residues have different environments in MHC class I and class II complexes, they both interact with a similar segment of helix H2b in α_2 or β_1 (see figure C, this page). The fourth hypervariable loop of Vα, CDR 4α, is able to switch a salt bridge from the conserved TCR Vα residue Lys^{68} to the equally highly conserved Glu^{166} α_2 in class I or the conserved Asp^{76} β_1 in class II, one helix turn away. Another class-specific salt bridge in the TCR D10 complex is formed on the Vβ side of the binding site where conserved Glu^{58} on CDR 2β reaches over and interacts with a highly conserved Lys^{39}, not from the MHC α_1 helix but from a conserved loop that connects the β strands, S3 and S4. Such pairs of salt bridges could certainly restrict the orientation of any TCR onto its particular class of MHC molecule. A real difference in Vα orientation could certainly influence binding of the TCR–peptide MHC complex to CD4 or CD8. The acidic binding loop for the coreceptor on MHC α_3 of class I and β_2 of class II is on the Vα side, although in quite distinct positions and orientations for the "fuzzy" set of class I versus class II conformations. So, the next major structural question to address is how the entire TCR-CD3-CD8 or CD4 signaling complex is assembled.

But, we should not overlook the need for more TCR–peptide MHC structures, both for class II and for class I. Until we can routinely predict with some accuracy how any given TCR sits on its peptide-MHC, we still have work to do. It took many, many antibody-antigen structures to glean the key molecular recognition principles of this interaction. Meanwhile, the new structure tells us a lot and, coupled with accomplishments of the recent nuclear magnetic resonance structure of TCR D10 (*10*), is a significant and much needed addition to the TCR structural database.

References and Notes

1. K. C. Garcia *et al.*, *Science* **274**, 209 (1996).
2. D. N. Garboczi *et al.*, *Nature* **384**, 134 (1996).
3. K. C. Garcia *et al.*, *Science* **279**, 1166 (1998).
4. Y. H. Ding *et al.*, *Immunity* **8**, 403 (1998).
5. M. K. Teng *et al.*, *Curr. Biol.* **8**, 409 (1998).
6. K. C. Garcia *et al.*, *Annu. Rev. Immunol.* **17**, 369 (1999).
7. P. M. Rudd *et al.*, *J. Mol. Biol.* **293**, 351 (1999).
8. E. L. Reinherz *et al.*, *Science* **286**, 1913 (1999).
9. B.-C. Sim *et al.*, *Immunol. Today* **19**, 276 (1998).
10. B. J. Hare *et al.*, *Nature Struct. Biol.* **6**, 574 (1999).
11. M. L. Connolly, *Science* **221**, 709 (1983).
12. T. E. Ferrin *et al.*, *J. Mol. Graphics* **6**, 13 (1988); C. C. Huang *et al.*, *J. Mol. Graphics* **9**, 230 (1991).
13. P. Kraulis, *J. Appl. Crystallogr.* **24**, 946 (1991).
14. D. J. Bacon and W. F. Anderson, *J. Mol. Graphics* **6**, 219 (1988); E. A. Merritt and M. E. P. Murphy, *Acta Crystallogr.* **D50**, 869 (1994).
15. I thank E. L. Reinherz, A. Smolyar, and J.-H. Wang for access to the D10 coordinates, and R. L. Stanfield and M. Yu for preparation of the figures.

http://www.jstor.org

LINKED CITATIONS

- Page 1 of 1 -

You have printed the following article:

Class-Conscious TCR?
Ian A. Wilson
Science, New Series, Vol. 286, No. 5446. (Dec. 3, 1999), pp. 1867-1868.
Stable URL:
http://links.jstor.org/sici?sici=0036-8075%2819991203%293%3A286%3A5446%3C1867%3ACT%3E2.0.CO%3B2-I

This article references the following linked citations:

References and Notes

[1] **An## T Cell Receptor Structure at 2.5 Å and Its Orientation in the TCR-MHC Complex**
K. Christopher Garcia; Massimo Degano; Robyn L. Stanfield; Anders Brunmark; Michael R. Jackson; Per A. Peterson; Luc Teyton; Ian A. Wilson
Science, New Series, Vol. 274, No. 5285. (Oct. 11, 1996), pp. 209-219.
Stable URL:
http://links.jstor.org/sici?sici=0036-8075%2819961011%293%3A274%3A5285%3C209%3AATCRSA%3E2.0.CO%3B2-2

[8] **The Crystal Structure of a T Cell Receptor in Complex with Peptide and MHC Class II**
Ellis L. Reinherz; Kemin Tan; Lei Tang; Petra Kern; Jin-huan Liu; Yi Xiong; Rebecca E. Hussey; Alex Smolyar; Brian Hare; Rongguang Zhang; Andrzej Joachimiak; Hsiu-Ching Chang; Gerhard Wagner; Jia-huai Wang
Science, New Series, Vol. 286, No. 5446. (Dec. 3, 1999), pp. 1913-1921.
Stable URL:
http://links.jstor.org/sici?sici=0036-8075%2819991203%293%3A286%3A5446%3C1913%3ATCSOAT%3E2.0.CO%3B2-L

[11] **Solvent-Accessible Surfaces of Proteins and Nucleic Acids**
Michael L. Connolly
Science, New Series, Vol. 221, No. 4612. (Aug. 19, 1983), pp. 709-713.
Stable URL:
http://links.jstor.org/sici?sici=0036-8075%2819830819%293%3A221%3A4612%3C709%3ASSOPAN%3E2.0.CO%3B2-T

NOTE: *The reference numbering from the original has been maintained in this citation list.*